Electronic Supplementary Material (ESI) for Dalton Transactions.
This journal is © The Royal Society of Chemistry 2023

Electronic Supporting Information

A layered $CoSeO_3$ pre-catalyst for electrocatalytic water oxidation

Ting Wang,[a] Shujiao Yang,[a] Haoquan Zheng,[a] Wei Zhang,[*a] and Rui Cao[*a]

Key Laboratory of Applied Surface and Colloid Chemistry, Ministry of Education, School of Chemistry and Chemical Engineering, Shaanxi Normal University, Xi'an 710119, China.

*Corresponding authors. Emails: zw@snnu.edu.cn (W.Z.); ruicao@snnu.edu.cn (R.C.).

General materials

K_2CO_3 (99.0%, Energy Chemical), $CoCl_3 \cdot 6H_2O$ (99.0%, Energy Chemical), $Co(SO_4) \cdot 7H_2O$ (99.0%, Energy Chemical), Co(OAc)2·$4H_2O$ (99.0%, Energy Chemical), SeO_2 (99.0%, Energy Chemical), KOH (98.0%, Energy Chemical), and Nafion (5 wt%, DuPont) were acquired from commercial supplies and used without further purification. Milli-Q water of 18 MΩ cm was used in all experiments unless otherwise stated.

The dependence of the reaction rate on the proton activity was derived based on the following Equation (S1):

$$\rho_{RHE} = \left(\frac{\partial E}{\partial pH}\right)_j = -\left(\frac{\partial E}{\partial \log(j)}\right)_{pH} \left(\frac{\partial \log(j)}{\partial pH}\right)_E$$

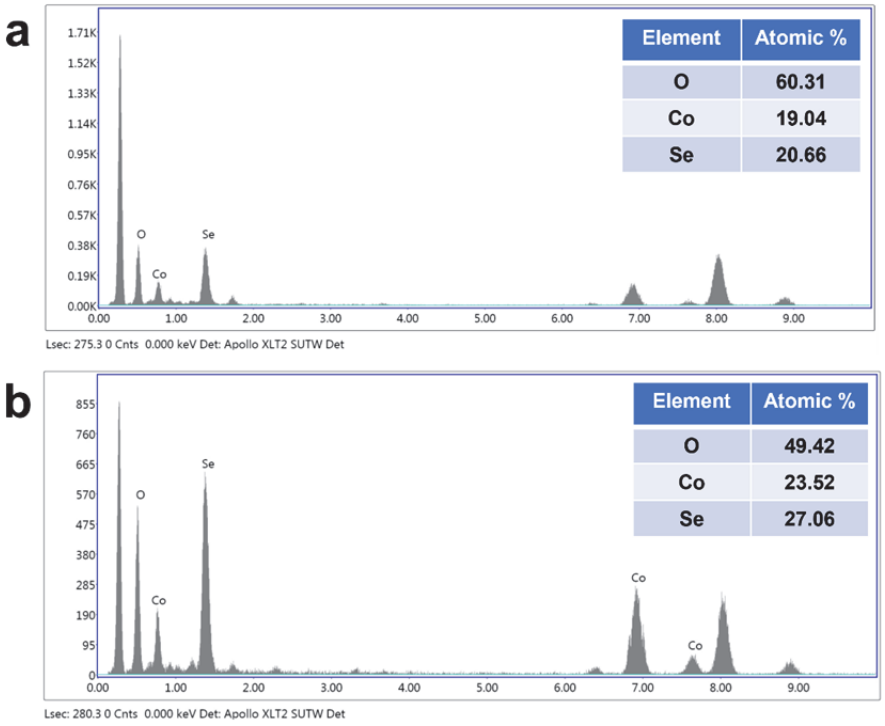

Figure S1. EDX spectra of (a) $CoSeO_3$ and (b) $CoSeO_3 \cdot 2H_2O$.

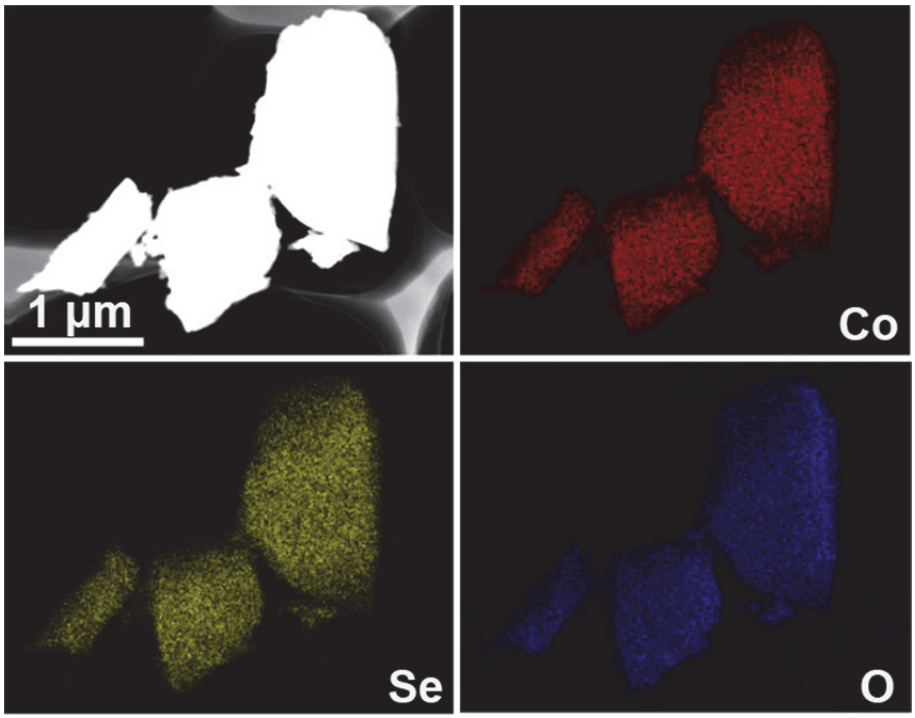

Figure S2. EDX elemental mapping images of Co, Se, and O for $CoSeO_3$.

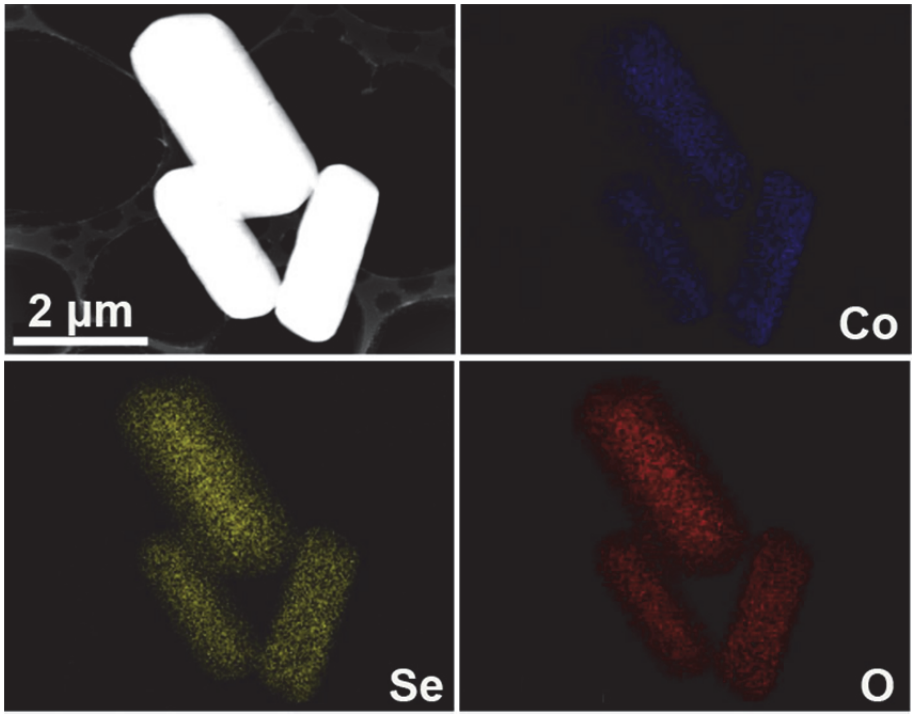

Figure S3. EDX elemental mapping images of Co, Se, and O for $CoSeO_3 \cdot 2H_2O$.

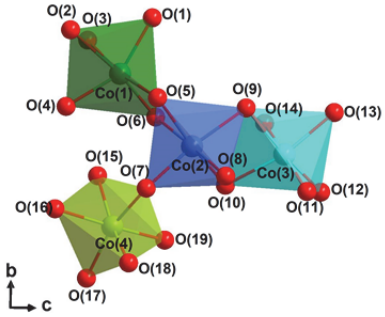

		Atom	Distance (Å)
$CoSeO_3$	$Co(1)O_6$	Co(1)-O(1)	2.0836
		Co(1)-O(2)	2.3439
		Co(1)-O(3)	2.2587
		Co(1)-O(4)	2.0399
		Co(1)-O(5)	2.0366
		Co(1)-O(6)	2.0488
	$Co(2)O_6$	Co(2)-O(5)	2.0448
		Co(2)-O(6)	2.2568
		Co(2)-O(7)	2.0183
		Co(2)-O(8)	2.2351
		Co(2)-O(9)	2.1320
		Co(2)-O(10)	2.1077
	$Co(3)O_6$	Co(3)-O(9)	2.1415
		Co(3)-O(10)	2.0999
		Co(3)-O(11)	2.1320
		Co(3)-O(12)	2.0528
		Co(3)-O(13)	2.0614
		Co(3)-O(14)	2.1615
	$Co(4)O_6$	Co(4)-O(7)	2.0706
		Co(4)-O(15)	2.0422
		Co(4)-O(16)	2.0748
		Co(4)-O(17)	2.0383
		Co(4)-O(18)	2.2597
		Co(4)-O(19)	2.1208

Figure S4. Crystal structure of Co-polyhedrons and bond lengths in $CoSeO_3$.

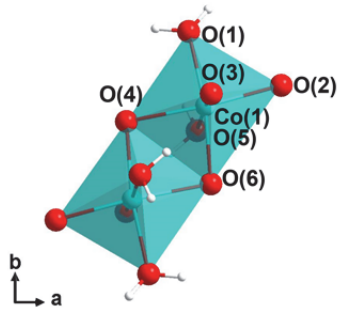

		Distance (Å)
$CoSeO_3 \cdot 2H_2O$	Co(1)-O(1)	2.0279
	Co(1)-O(2)	2.0589
	Co(1)-O(3)	2.1484
	Co(1)-O(4)	2.1051
	Co(1)-O(5)	2.1577
	Co(1)-O(6)	2.0610

Figure S5. Crystal structure of Co-polyhedrons and bond lengths in $CoSeO_3 \cdot 2H_2O$.

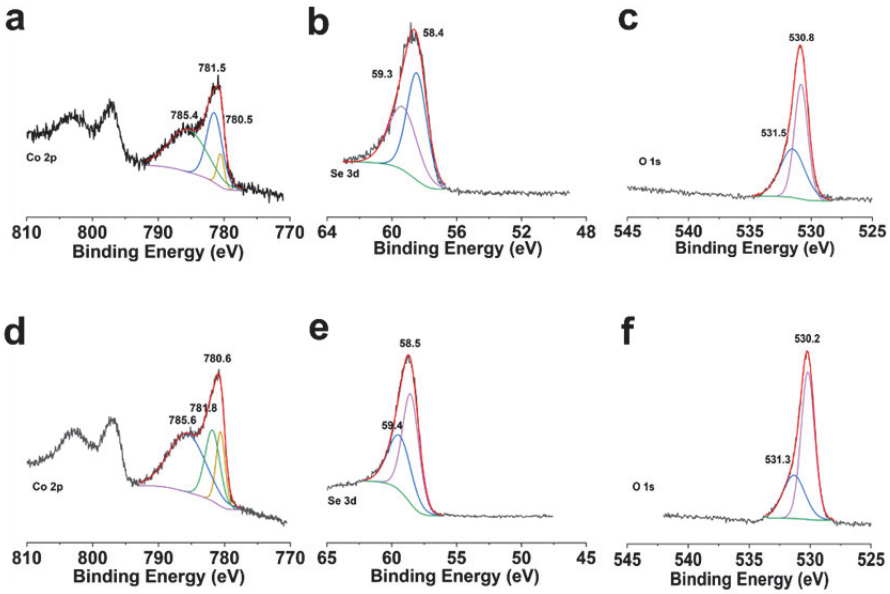

Figure S6. XPS spectra of (a-c) $CoSeO_3$ and (d-f) $CoSeO_3 \cdot 2H_2O$ in the Co 2p, Se 3d, and O 1s regions.

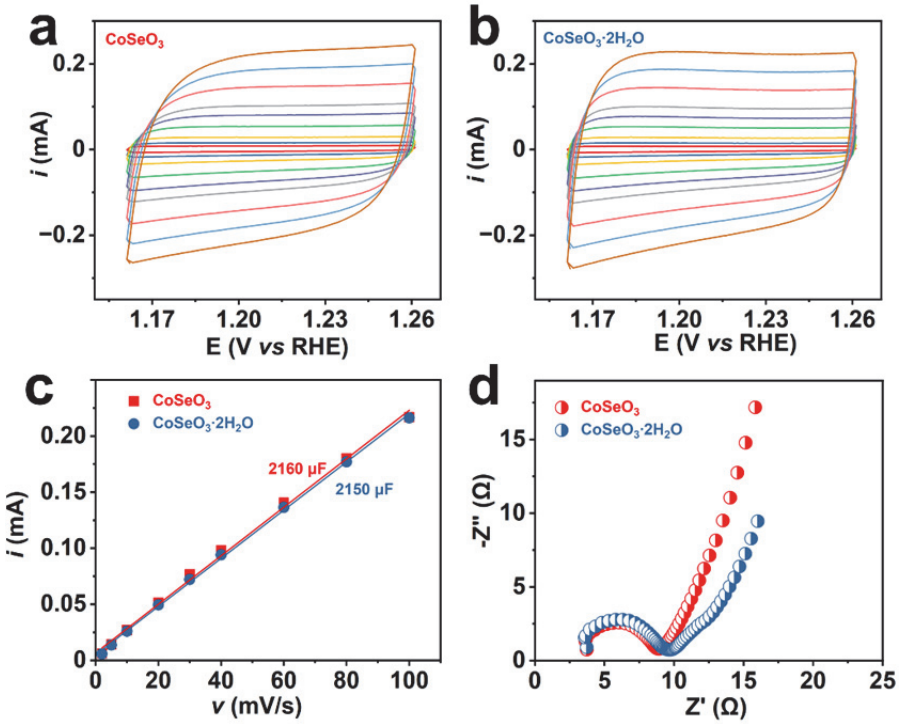

Figure S7. The charging-discharging currents of (a) $CoSeO_3$ and (b) $CoSeO_3{\cdot}2H_2O$ collected in the non-Faradaic potential range with scan rates of 2, 5, 10, 20, 30, 40, 60, 80, and 100 mV s^{-1}. (c) The charging currents plotted against the scan rates, the slope of which represents the electrochemical surface capacitances. (d) Nyquist plots of $CoSeO_3$ and $CoSeO_3{\cdot}2H_2O$ at OCP.

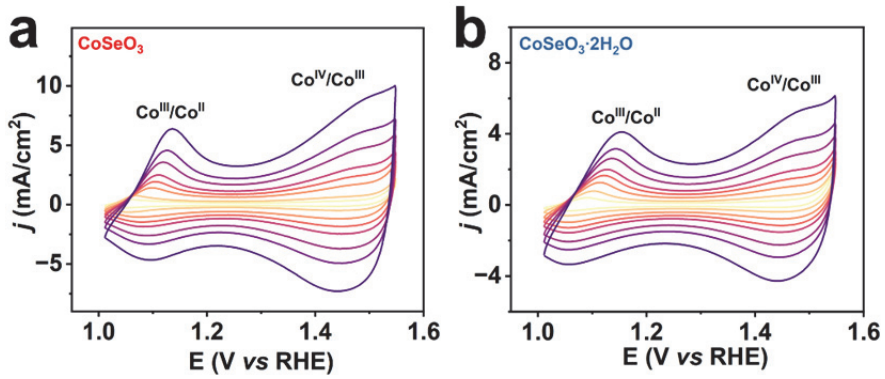

Figure S8. CV curves at different scan rates (2, 5, 10, 15, 20, 30, 40, and 60 mV s^{-1}) of (a) $CoSeO_3$ and (b) $CoSeO_3 \cdot 2H_2O$.

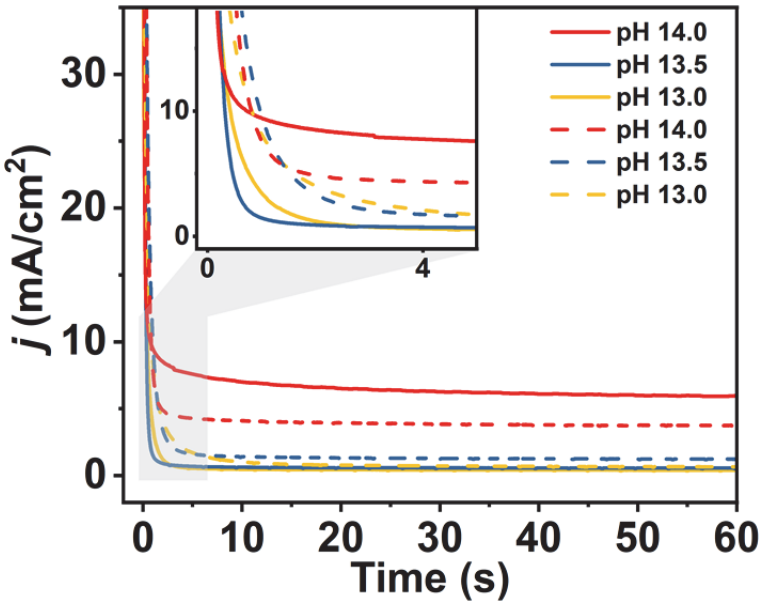

Figure S9. Chronoamperograms of $CoSeO_3$ and $CoSeO_3 \cdot 2H_2O$ at different pH values (14.0, 13.5, and 13.0) at a constant bias of 0.560 V (*vs* Ag/AgCl). The Solid lines represent $CoSeO_3$ and the dashed lines represent $CoSeO_3 \cdot 2H_2O$.

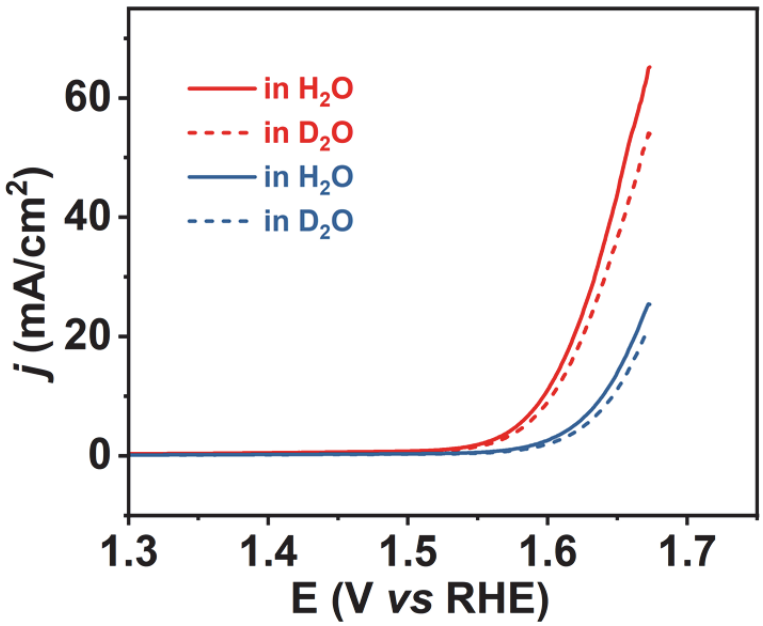

Figure S10. The LSV curves of $CoSeO_3$ (red) and $CoSeO_3 \cdot 2H_2O$ (blue) in H_2O and D_2O solutions.

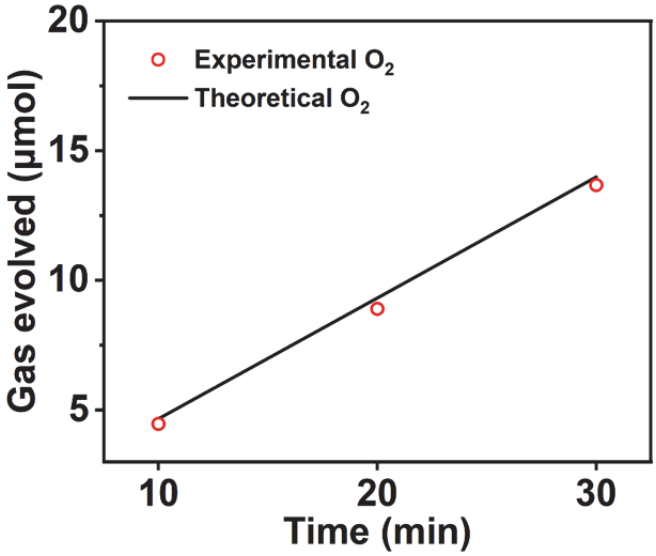

Figure S11. Experimental (from gas chromatography analysis) and theoretical (from transferred charge) amount of O_2 evolved by the chronopotentiometry with $CoSeO_3$ catalyst for OER at 3 mA. The faradaic efficiency is > 95%.

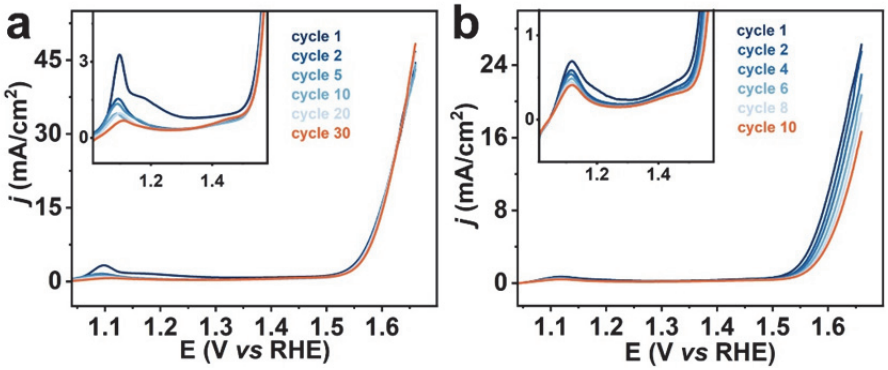

Figure S12. LSV curves for (a) $CoSeO_3$ and (b) $CoSeO_3 \cdot 2H_2O$ after water oxidation activation.

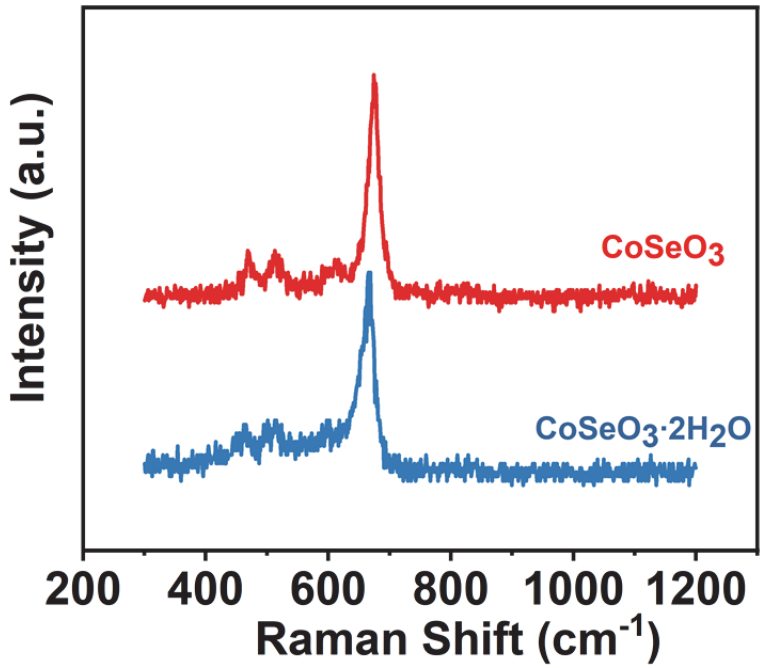

Figure S13. Raman spectra of $CoSeO_3$ and $CoSeO_3 \cdot 2H_2O$ acquired after OER.

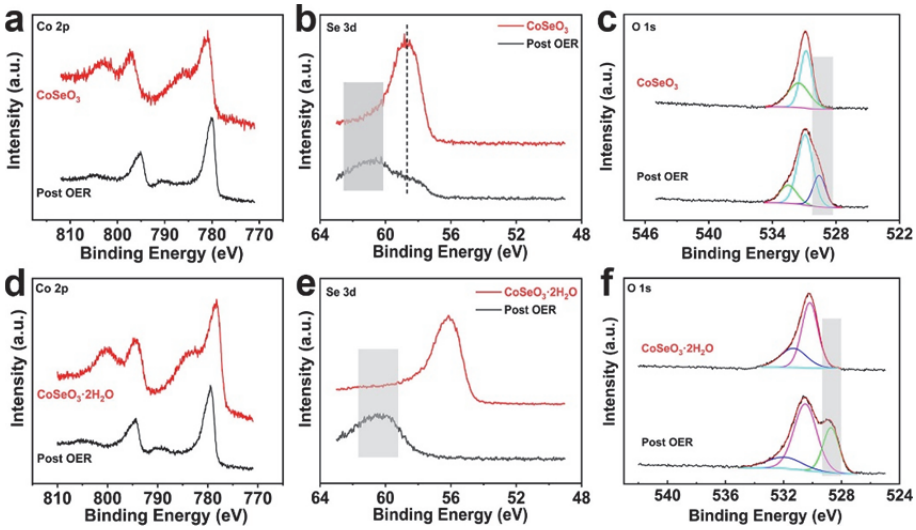

Figure S14. XPS spectra of (a-c) $CoSeO_3$ and (d-f) $CoSeO_3 \cdot 2H_2O$ of in the Co 2p, Se 3d, and O 1s regions acquired before and after OER.

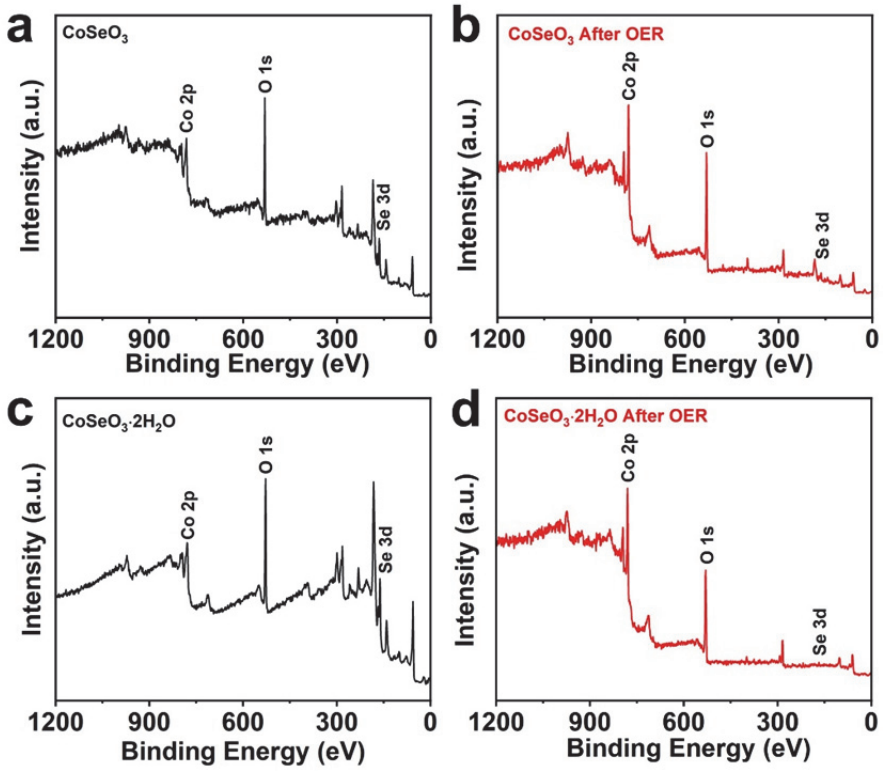

Figure S15. XPS survey scan spectra of (a, b) $CoSeO_3$ and (c, d) $CoSeO_3 \cdot 2H_2O$ before and after OER electrolysis.

Table S1. The contents of Se in $CoSeO_3$ and $CoSeO_3 \cdot 2H_2O$ samples before and after OER determined by XPS analysis.

	Se 3d/At% (Before OER)	**Se 3d/At% (After OER)**
$CoSeO_3$	18.02	6.26
$CoSeO_3 \cdot 2H_2O$	24.97	1.33

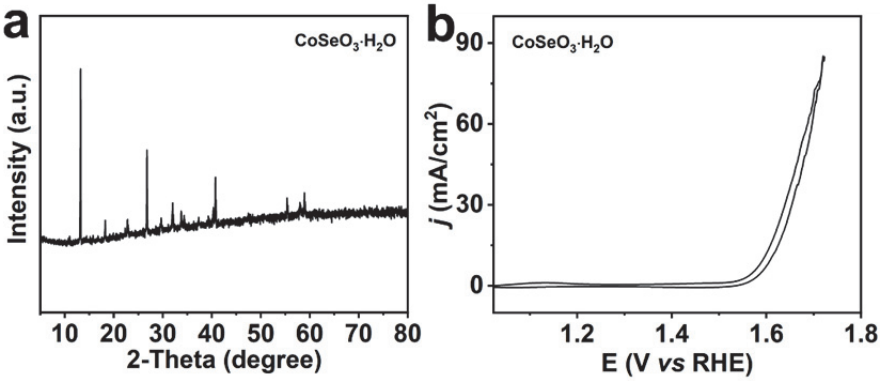

Figure S16. (a) XRD pattern of $CoSeO_3 \cdot H_2O$. (b) CV curve of $CoSeO_3 \cdot H_2O$ in 1 M KOH solution.

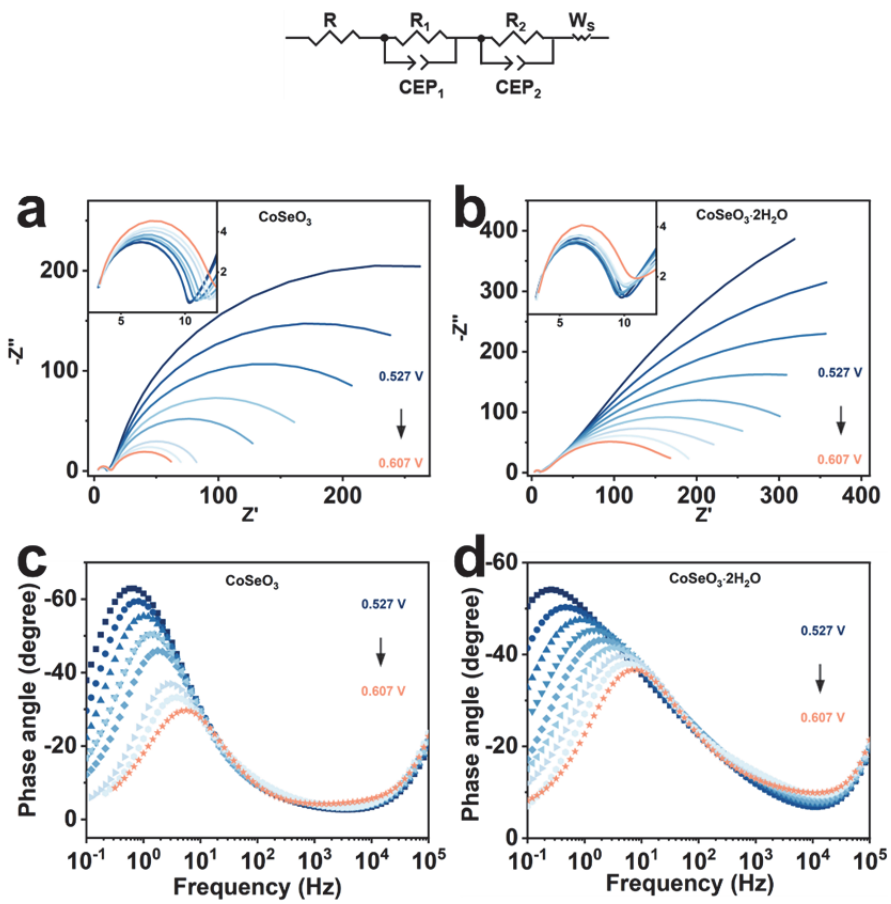

Figure S17. Nyquist plots of (a) $CoSeO_3$ and (b) $CoSeO_3 \cdot 2H_2O$ acquired at different potentials (0.527, 0.537, 0.547, 0.557, 0.567, 0.577, 0.587, 0.597, and 0.607 V (*vs* Ag/AgCl)) in 1.0 M KOH. (c, d) The corresponding Bode plot showing phase data. Data is fitted to a modified Randle's circuit.

Table S2. Comparison of the electrocatalytic OER performance for $CoSeO_3$ and other reported $MSeO_x$–based electrocatalysts.

Catalysts	Substrates	Electrolyte	Overpotential (@10 mA/cm^{-2})	Reference
$CoSeO_3$	**GC**	**1.0 M KOH**	**350 mV**	**This work**
$CoSeO_3 \cdot 2H_2O$	**GC**	**1.0 M KOH**	**400 mV**	**This work**
$CoSe_2$	CC	1.0 M KOH	432 mV	*J. Phys. Chem. C*, 2020, **124**, 9673–9684.
MOF $CoSeO_3$	NF	1.0 M KOH	290 mV (@50 mA/cm^{-2})	*Inorg. Chem.*, 2020, **59**, 3817–3827.
$CoSeO_3 \cdot H_2O$	FTO	1.0 M KOH	310 mV	*Energy Environ. Sci.*, 2020, **13**, 3607–3619.
$Mn_3O_4/CoSe_2$	GC	0.1 M KOH	450 mV	*J. Am. Chem. Soc.*, 2012, **134**, 2930–2933.
PdO@$CoSe_2$	GC	1.0 M KOH	260 mV (@20 mA/cm^{-2})	*RSC Adv.*, 2023, **13**, 743–755.
$CoSe_2$/N-Graphene	CF	0.1 M KOH	366 mV	*ACS Nano*, 2014, **8**, 3970–3978.
$CoSe_2$-CeO_2	GC	0.1 M KOH	288 mV	*Small*, 2015, **11**, 182–188.
$FeSe_2/CoSe_2$@SC	GC	1.0 M KOH	407 mV	*Electrochim. Acta*, 2023, **445**, 142049.
Ni_3Se_4/UCL-3	GC	1.0 M KOH	350 mV	*Chem. Eng. J.*, 2022, **430**, 132720.
FeSe/NC-PoFeSe	GC	0.1 M KOH	330 mV	*ACS Appl. Mater. Interfaces,* 2018, **10**, 32133–32141.
MnSe	GC	1.0 M KOH	310 mV	*J. Mater. Chem. A*, 2022, **10**, 6772–6784.